Fabrication of copper patterns on industrial-used dielectric substrates by direct laser metallization from deep eutectic solvents

Ekaterina A. Avilova [1], Evgeniia M. Khairullina [2], Andrey Yu. Shishov [2], Elizaveta A. Eltysheva [1], Margarita A. Zaikina [1], Dmitry A. Sinev [1], Ilya I. Tumkin [3,*]

[1] School of Physics and Technology, ITMO University, 197101 St. Petersburg, Russia.

[2] Institute of Chemistry, Saint Petersburg State University, 199034 St. Petersburg, Russia.

[3] Ruhr-Universität Bochum, Bochum, Germany

* Ilia.Tumkin@ruhr-uni-bochum.de

Abstract

In this study, we show the possibilities of developing a method for manufacturing electrically conductive copper patterns of arbitrary topology on various dielectric substrates by laser-induced synthesis from deep eutectic solvents. The possibility of printing on the industrially demanded dielectrics is shown, e.g., on polyimide, fiberglass plastic, and polytetrafluoroethylene (PTFE) substrates. The geometric and electrical properties of the resulting structures, as well as their composition, have been studied. The influence of the substrate material is shown to be substantial for the effective rate of formation of structures and their final properties.

Keywords: direct laser metallization; copper; flexible electronics; deep eutectic solvents

Introduction

In recent years, the flexible electronics industry field has been under an active development, especially due to the potential to create and integrate in such areas as wearable electronics [1,2], health and medical sciences [3,4], sensorics [5,6,7], automotive [8], energy storage [9], etc. Unfortunately, to this day most applications and devices have been manufactured by using decades-old processes for the fabrication of microelectronic components. Usage of mature technologies could be cost-effective to some extent, but at the same time potential refurbishment costs are limiting the development of new materials and innovative techniques.

The polyimide and fiberglass are used widely as substrates for electronic components in various applications [10,11], while the fabrication of metal structures on the surface of polytetrafluoroethylene (PTFE) is a challenge to the scientific world, due to the high chemical resistance and poor adhesion of metals to this surface [12,13,14]. However, the advantages of PTFE application in the field of printed circuit board (PCB) fabrication for ultra-high frequency electronics are undisputable due to its high damage resistance. Thus, the development of unified approaches and technologies that can be applied both to rigid dielectrics and to the relatively fragile and flexible materials utilized in the production of flexible electronics is an extremely urgent task [15,16].

Therefore, in recent years, methods of direct laser writing (DLW) have been developed rapidly, and soon may provide a significant technological step in microelectronics manufacturing. In comparison with alternative microfabrication techniques (e.g., photolithography [17,18], inkjet printing [19], and screen printing [20]) DLW has a number of advantages, for example, high localization spatial resolution, environment friendliness,

fast processing rate, and the possibility to plating a wide range of materials like glass [21,22], polymers [22,23], paper or other fragile carbon-based materials 24], etc. . Compared to traditional manufacturing methods, it is proven to be flexible and effective, exhibiting particularly good ability and processing quality when recording sophisticated and complex structures with high reproducibility.

Hence, laser-assisted metallization techniques can be classified as a group of approaches where various types of precursor combinations are used and pre-treatment or chemical treatment steps are required [25,26]. For example, in [27] and [28], a comprehensive investigation of reductive laser sintering technique for fabricating micro-thermocouples, and also tactile and electrochemical sensors [29,30] has been performed. These works have demonstrated the fabrication of copper, nickel and metal oxide films on the surface of a wide range of polymer materials.

Also, the approaches [31,32,33], where the first step is surface activation by laser radiation and then chemical metallization, demonstrated the potential of this technology to fabricate electrochemical sensors and other devices.

Laser-induced selective metallization (LISM) is a method of interest, the principal steps of which involve the fabrication of a patterns by mixing a polymer with laser sensitizers and then, after laser activation and electrolytic coating, metallic patterns are being successfully fabricated on the laser-activated surface [34,35,36]. However, limitations of such methods consist in high cost of equipment and precursors, the necessity of preliminary surface activation stages, and in the case of LISM, the preparation of a composite for irradiation.

Among DLW techniques worth noting the direct laser metallization (DLM) technology, which focuses on the precise selection and synthesis of a precursor that is irradiated with laser light of a certain intensity and pulse duration, leading to a chemical reaction and the formation of a metallic micropattern on the surface [23,37,38]. For example, it has been shown that DLM can be successfully utilized to fabricate copper, nickel, gold, and other metal-based micro-patterns on glass and ceramic surfaces [39,40,41]. Since precursor preparation for many nanomaterials might be complicated and time consuming, further development of the DLM method led to finding the new types of precursors that are cheap, environmentally friendly, and can be easily synthesized. It has been shown that deep eutectic solvents (DES), which have previously been demonstrated as effective extractants in analytical chemistry [42] as well as media for electrochemical metallization [43], can potentially take the place of the sought-for precursor.

We have previously shown the metallization of glass surfaces using DES based on choline chloride, citric and tartaric acids, and copper chloride and acetate [44]. However, in that work, CW laser was applied and in the treatment of polymer materials, a significant temperature effect led to melting or graphitization of the surface. In [45] an effective solution for metallization of glass surfaces was achieved by using a commercially available MiniMarker-2, however, the applicability of the developed methods for wider substrate materials range remained unknown.

In the present work, the proposed approach has been extended and significantly modified, in particular for metallization of a wide range of materials widely utilized in the microelectronics industry.

Methods & Materials

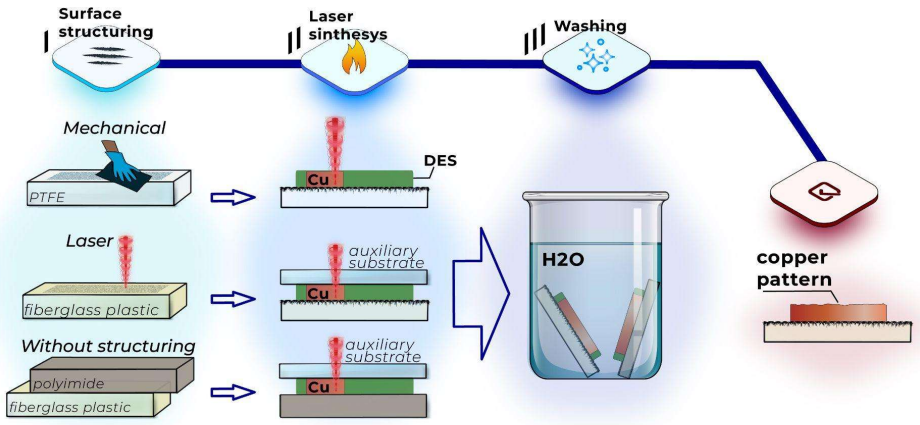

Fig. 1 Laser-induced deposition technique.

To create the DES, choline chloride, tartaric acid, and copper acetate were placed into a 20 mL glass vial and heated in the drying cabinet at 120 °C for approximately 10–15 min. Once the mixture started to liquefy visibly, the forming DES was placed in a heating magnetic stirrer at 130 °C and stirred for 40 min until complete homogeneity was achieved.

In our research various acceptor substrate materials were used for laser-induced Cu deposition from DES, namely 1.0 mm thick borosilicate glass (Micromed, Observation devices LLC., St. Petersburg, Russia), 0.1 mm thick polyimide (PL) (Izolit-SPb LLC., St. Petersburg, Russia), 1.0 mm thick fiberglass plastic (FG plastic) (Izolit-SPb LLC., St. Petersburg, Russia), and 1.0 mm thick polytetrafluoroethylene (PTFE) (Profizolit LLC., St. Petersburg, Russia). These substrate materials were chosen for their wide usage in the production of printed circuit boards and integrated circuits. All the substrates were rinsed in the isobutyl alcohol and distilled water to avoid contamination before DES application. Pre-treatment procedure for borosilicate glass substrates before forming structures was presented in more detail in our previous article [45], and consisted of laser-assisted structuring (laser-induced plasma-assisted ablation method, LIPAA [46,47,48]) to create an additional roughness and a layer of ablation products on the acceptor surface. Substrates made of fiberglass plastic and PTFE were also structured before rinsing to create an additional roughness Ra of the order of 7 μm (mechanically with 320 P sandpaper) in order to increase the further adhesion of the Cu layers. The polyimide substrate was not pre-treated, since it was determined during the studies that, despite the apparent chemical inertness [49,50,51], this material has sufficient adhesion and can be effectively metallized using the method under study.

After the structuring stage for glass and after the cleaning stage for other materials, a 1 mm thick layer of DES was applied on the prepared substrate. Earlier [45] we have shown an effective usage of an auxiliary glass slab placed onto DES layer to create a “sandwich” sample, which was used for borosilicate glass, polyimide and fiberglass plastic processing in current research. Finally, the prepared sample was placed in the processing plane of a MiniMarker-2 (Laser Center LLC, St. Petersburg, Russia) Yb-fiber laser setup, and irradiated by laser beam with wavelength 1070 nm, pulse duration 200 ns, pulse repetition rate 20 kHz, and average power up to 20 W. Average power P, pulse repetition frequency f, scanning speed V, and number of repetitive exposures N varied in this research.

Optical microscopy (Carl Zeiss Axio Imager A1.m, Carl Zeiss Microscopy GmbH, Munich, Germany), scanning electron microscopy (SEM, Hitachi S-3400N), energy-dispersive X-ray spectroscopy (EDX-AzTec Energy 350, Oxford Instruments, Abingdon, UK), Raman spectroscopy (SENTERRA, Bruker Corporation, USA) were used to analyze the geometrical, physical, and chemical properties of the structures. Temperature analysis was conducted using a thermal imaging camera FLIR Titanium 520M.

Results and discussion

The recording conditions for fabrication of conductive structures on the abovementioned substrate were optimized (Fig.2). Polyimide and fiberglass showed an expectedly higher affinity to the recorded structures than PTFE, allowing copper tracks formation with laser power P 3.9 W and 4.7 W, scanning speed V = 0.8 – 1.2 mm/s and V = 2 – 14 mm/s respectively, and number of consequent exposures N 1-4 (yielding the resulting effective speed Veff = V/N to 1 – 3.5 mm/s), contra to P = 3.1 W, V = 20 mm/s, and N = 40 consequent exposures (Veff = 0.5 mm/s) necessary for recording on PTFE.

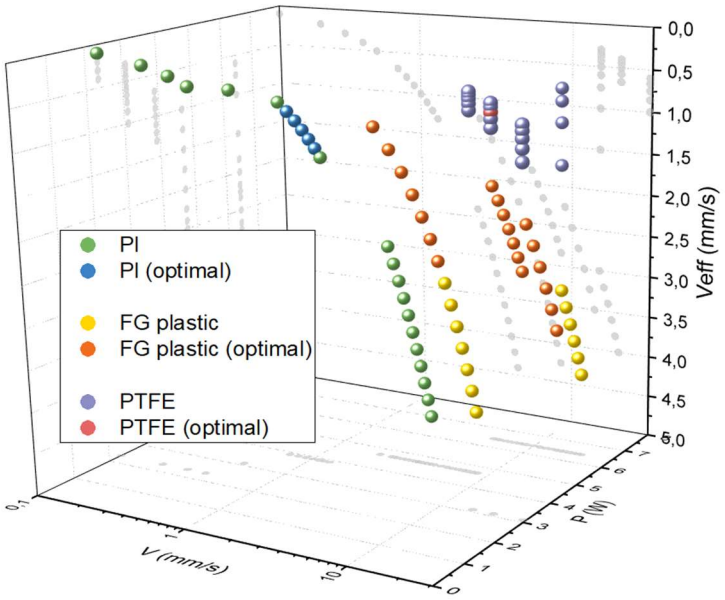

Fig. 2 Recording regimes for the organic substrates under study. The effective speed Veff is defined as the scan speed V divided by the number of exposures N.

For the formation of continuous conductive structures without defects (e.g., uneven deposition, chips, cracks, etc.), sufficient adhesion of the restored metal to the substrate is required, which is especially evident when depositing on the PTFE substrates. It has been shown that the formation of copper structures is unlikely unless the substrate was pre-treated for additional roughening, which apparently served as convenient crystallization centers for the recovering copper. This notion was also confirmed by the copper deposition not on the PTFE substrate, but rather on the auxiliary glass, when one was used in the experiment. Roughening was achieved by grinding the substrate with sandpaper, which resulted in copper structures formation at Veff about 0.5 mm/s. Although the copper layers recorded under these conditions are thin and fragile, when trying to increase the layer thickness by longer exposure, it fragments and splits off the substrate during bending or carrying out the contact measurements.

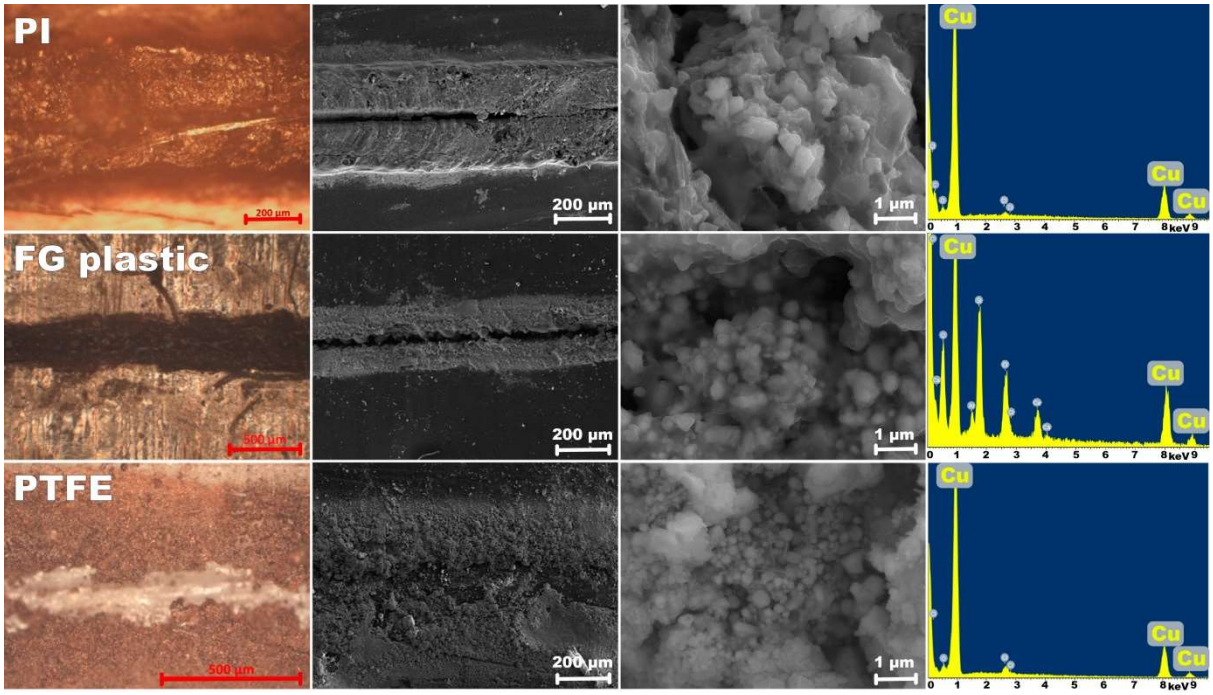

Fig. 3 Optical (first column), scanning electron (second and third columns) and energy dispersive X-ray (fourth column) microscopy for the structures on PI, FG plastic and PTFE substrates.

The formation of tracks both on PTFE and fiberglass was possible only with several sequential exposures by the same trajectory. In our previous studies of copper deposition on glass repeated exposures allowed the formation of a thicker and more uniform layer [45], but for the polymer substrates in this study, single exposures lead to copper fixing to the substrate in sketchy areas. Although the effective speed for copper tracks formation on fiberglass (3.5 mm/s) is about the same order with the reference speed for recording on glass (2 mm/s).The copper layers adhesion is high, but those layers tend to oxidize faster than usual, probably due to thermally-induced structural and chemical changes in the epoxy resin consisting in the fiberglass.

The surface resistance of the structures on each substrate was measured by the two-probe method, which is suitable for conductors with a thickness less than the distance between the measuring probes (1 mm). The thickness (height) of all measured structures did not exceed 50 µm, and thus the measured values of the surface resistance were converted into the resistivity for comparison (Table 1). It was not possible to measure the resistivity of the structures formed on the PTFE as they tended to fragment at the contact measurements. The resistivity of the structure on the polyimide substrate is almost 100 times higher than the reference value for pure copper, apparently, due to significant oxidation occurring with long-term interaction of the already formed structure and oxygen in the heated air pockets formed due to the hydrodynamic redistribution of DES during laser processing. Resistance raise could be also possibly connected to the formation of an inhomogeneous, porous structure with the inclusion of a large amount of carbon and other impurities due to thermally-induced ablation of the substrate (Fig 3). The tracks formation on fiberglass is also linked with a partial disruption of the substrate, which is evident from the presence of Al2O3 and Si in the tracks according to the EDX results (Fig 3).

Table 1 Recorded samples resistivity.

	Pure copper (reference) [52]	Structure on glass	Structure on fiberglass	Structure on polyimide	Structure on PTFE

Resistivity, Ω x mm²/m	0.0172	0.0253	0.2267	1.6354	N/A

Worth noting that the oxygen presence in the recorded structures, which may indicate the formation of copper oxides, also confirmed by the Raman shift (Fig 4). Copper oxides occur in air usually at temperatures higher than 200°C [53,54,55,56], but our previous results achieved on glass substrates in temperature range of 23-237 °C showed no signs of oxidation [45]. Measured average temperatures in the current study were significantly below 240 °C for all the organic substrates (Fig. 5), but the resulting structures still were oxidized, which was confirmed by the Raman measurements and visually based on a characteristic darkening. Thus, the oxidation could be considered to be a result of the organic substrate influence, decomposing under laser action into compounds more active than mostly chemically neutral constituents of glass. Important to note that the temperature was recorded using thermal imaging with a resolution of about 20 μm, due to which the temperature value averaged over a 20x20 μm area was obtained. Also, the time resolution of the equipment used allowed us to resolve frames with a time interval of at least 100 ms. Relaxation temperature changes in the case of using nanosecond pulses are much faster, which is why it can be only assumed that the peak values achieved are much higher and cross the thresholds of copper oxidation, which is just indicated by Raman shift.

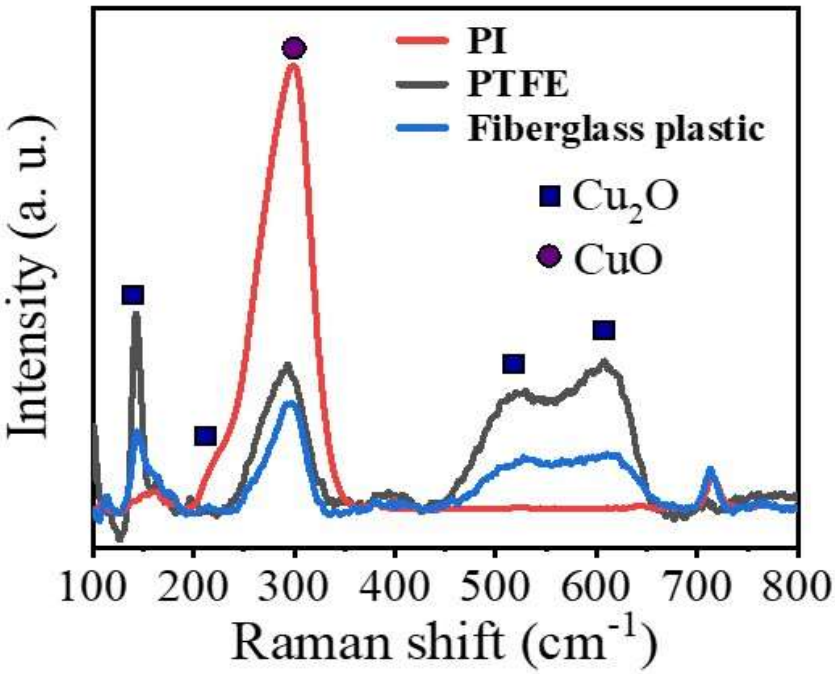

Fig. 4 Raman scattering spectra for the structures formed on PI, FG plastic and PTFE.

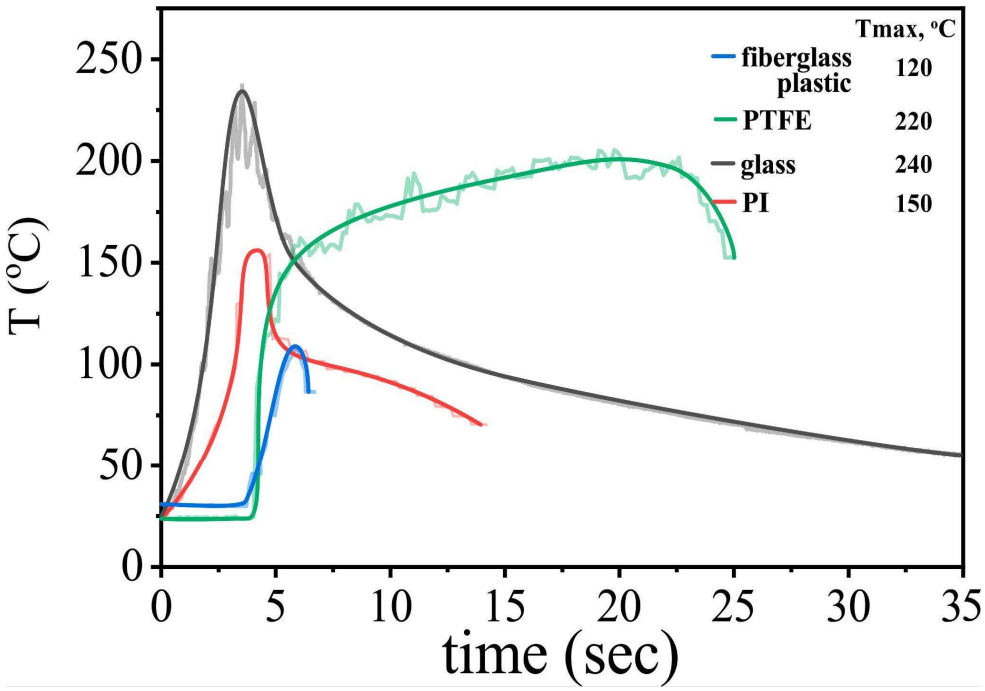

Fig. 5 Dynamics of the average temperature measured at a point on the scan axis.

As the most optimal material for the method used, a fiberglass substrate was chosen, on the surface of which conductive elements of printed circuit boards were formed (figure 6).

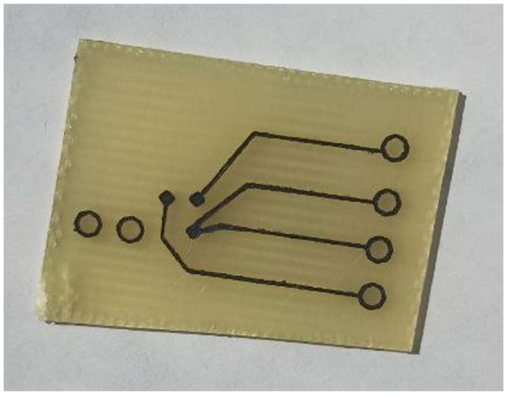

Fig. 6 Conductive elements of printed circuit boards formed on the FG substrate with P = 3.1 W, V = 10 mm/s, N = 20.

Conclusions

We found the parameters for creating micro-patterns on the surface of polyimide, PTFE, and fiberglass. For this purpose, a donor substrate was pre-structured, which allowed further formation of copper microcontacts with resistivity similar to pure copper. As a result, the laser regimes required to fabricate micro-patterns with desired properties on the surface of selected materials were determined, and it could be a promising technology for industrial application.

The formation of structures on fiberglass is in many aspects similar to the processes of deposition on glass, however, the increased chemical activity of resins leads to more active oxidation. This material is characterized by high effective rates of formation of conductive structures with high adhesion (about 3.5 mm/s). Polyimide is characterized by relatively low rates of formation of conductive structures with high adhesion (of the order of 1 mm/s). PTFE does not allow the formation of conductive structures by laser-induced deposition

from DES, since the resulting structures do not have adhesion to the substrate, as a result of which they are easily destroyed.

In the case of deposition on polyimide and PTFE, the subsurface layer of the substrates is destroyed, the products of which are introduced into the formed structures, due to which their composition is disturbed and, consequently, the conductive characteristics deteriorate (higher resistance). Oxidation of the formed structures with the formation of Cu_2O and CuO oxides was also noted, which indicates temperatures above 350 °C. However, the formation of structures on glass occurred in approximately similar temperature ranges and only metallic copper was present in the composition. From this observation, it was concluded that more active oxidation occurs due to the influence of the substrates: their ablation, melting, and also the release of gases in the process of interaction with laser radiation.

References

[1] Zhou, X., Guo, W., Yao, Y., Peng, R., & Peng, P. (2021). Flexible Nonenzymatic Glucose Sensing with One-Step Laser-Fabricated Cu2O/Cu Porous Structure. Advanced Engineering Materials, 23(6), 2100192.

[2] Yang, Y., Song, Y., Bo, X., Min, J., Pak, O. S., Zhu, L., ... & Gao, W. (2020). A laser-engraved wearable sensor for sensitive detection of uric acid and tyrosine in sweat. Nature biotechnology, 38(2), 217-224.

[3] Someya, T., Sekitani, T., Iba, S., Kato, Y., Kawaguchi, H., & Sakurai, T. (2004). A large-area, flexible pressure sensor matrix with organic field-effect transistors for artificial skin applications. Proceedings of the National Academy of Sciences, 101(27), 9966-9970.

[4] Zhou, X., Guo, W., Yao, Y., Peng, R., & Peng, P. (2021). Flexible Nonenzymatic Glucose Sensing with One-Step Laser-Fabricated Cu2O/Cu Porous Structure. Advanced Engineering Materials, 23(6), 2100192.

[5] Klyamer, D., Shutilov, R., & Basova, T. (2022). Recent Advances in Phthalocyanine and Porphyrin-Based Materials as Active Layers for Nitric Oxide Chemical Sensors. Sensors, 22(3), 895.

[6] Zhou, X., Guo, W., Fu, J., Zhu, Y., Huang, Y., & Peng, P. (2019). Laser writing of Cu/CuxO integrated structure on flexible substrate for humidity sensing. Applied Surface Science, 494, 684-690.

[7] Toh, H. S., Batchelor-McAuley, C., Tschulik, K., & Compton, R. G. (2013). Electrochemical detection of chloride levels in sweat using silver nanoparticles: a basis for the preliminary screening for cystic fibrosis. Analyst, 138(15), 4292-4297.

[8] Loher, T., Seckel, M., Pahl, B., Bottcher, L., Ostmann, A., & Reichl, H. (2008, October). Highly integrated flexible electronic circuits and modules. In 2008 3rd International Microsystems, Packaging, Assembly & Circuits Technology Conference (pp. 86-89). IEEE.

[9] Linnemann, J., Taudien, L., Klose, M., & Giebeler, L. (2017). Electrodeposited films to MOF-derived electrochemical energy storage electrodes: a concept of simplified additive-free electrode processing for self-standing, ready-to-use materials. Journal of Materials Chemistry A, 5(35), 18420-18428.

[10] Zou, S., Mu, Y., Pan, B., Li, G., Shao, L., Du, J., & Jin, Y. (2022). Mechanical and biological properties of enhanced porous scaffolds based on triply periodic minimal surfaces. Materials & Design, 219, 110803.

[11] Zhang, S. J., Liu, Y. Y., Lv, S. S., Cheng, J. P., Liao, B., Pang, P., ... & He, L. (2022). Surface metallization of PTFE and PTFE composites by ion implantation for low-background electronic substrates in rare-event detection experiments. Nuclear Science and Techniques, 33(7), 90.

[12] Kothuru, A., Singh, A. P., Varaprasad, B. K. S. V. L., & Goel, S. (2020). Plasma TREATMENT and copper metallization for reliable plated-through-holes in microwave PCBS for space electronic packaging. IEEE Transactions on Components, Packaging and Manufacturing Technology, 10(11), 1921-1928.

[13] Łowkis, B., Ziaja, J., Klaus, P., & Krawczyk, D. (2020). Effect of magnetron sputtering parameters on dielectric properties of PTFE foil. IEEE Transactions on Dielectrics and Electrical Insulation, 27(3), 837-841.

[14] Mirshojaeian Hosseini, M. J., & Nawrocki, R. A. (2021). A review of the progress of thin-film transistors and their technologies for flexible electronics. Micromachines, 12(6), 655.

[15] Liao, J., Guo, W., & Peng, P. (2021). Direct laser writing of copper-graphene composites for flexible electronics. Optics and Lasers in Engineering, 142, 106605.

[16] Biswas, S., Schoeberl, A., Hao, Y., Reiprich, J., Stauden, T., Pezoldt, J., & Jacobs, H. O. (2019). Integrated multilayer stretchable printed circuit boards paving the way for deformable active matrix. Nature Communications, 10(1), 4909.

[17] Liu, W., Wang, J., Xu, X., Zhao, C., Xu, X., & Weiss, P. S. (2021). Single-step dual-layer photolithography for tunable and scalable nanopatterning. Acs Nano, 15(7), 12180-12188.

[18] Lee, S., Wajahat, M., Kim, J. H., Pyo, J., Chang, W. S., Cho, S. H., ... & Seol, S. K. (2019). Electroless deposition-assisted 3D printing of micro circuitries for structural electronics. ACS applied materials & interfaces, 11(7), 7123-7130.

[19] Xie, J. Q., Ji, Y. Q., Kang, J. H., Sheng, J. L., Mao, D. S., Fu, X. Z., ... & Wong, C. P. (2019). In situ growth of Cu (OH) 2@ FeOOH nanotube arrays on catalytically deposited Cu current collector patterns for high-performance flexible in-plane micro-sized energy storage devices. Energy & Environmental Science, 12(1), 194-205.

[20] Jo, S., Akin, S., Park, M. S., & Jun, M. B. G. (2022). Selective metallization on glass surface by laser direct writing combined with supersonic particle deposition. Manufacturing Letters, 31, 64-68.

[21] Lipateva, T., Lipatiev, A., Lotarev, S., Shakhgildyan, G., Fedotov, S., & Sigaev, V. (2022). One-Stage Femtosecond Laser-Assisted Deposition of Gold Micropatterns on Dielectric Substrate. Materials, 15(19), 6867.

[22] Ji, Y., Zhang, Y., Zhu, J., Geng, P., Halpert, J. E., & Guo, L. (2023). Splashing-Assisted Femtosecond Laser-Activated Metal Deposition for Mold-and Mask-Free Fabrication of Robust Microstructured Electrodes for Flexible Pressure Sensors. Small, 2207362.

[23] Peng, P., Li, L., He, P., Zhu, Y., Fu, J., Huang, Y., & Guo, W. (2019). One-step selective laser patterning of copper/graphene flexible electrodes. Nanotechnology, 30(18), 185301.

[24] Cantarella, G., Madagalam, M., Merino, I., Ebner, C., Ciocca, M., Polo, A., ... & Lugli, P. (2023). Laser-Induced, Green and Biocompatible Paper-Based Devices for Circular Electronics. Advanced Functional Materials, 2210422.

[25] Rytlewski, P., Jagodziński, B., Malinowski, R., Budner, B., Moraczewski, K., Wojciechowska, A., & Augustyn, P. (2020). Laser-induced surface activation and electroless metallization of polyurethane coating containing copper (II) L-tyrosine. Applied Surface Science, 505, 144429.

[26] Nam, V. B., Giang, T. T., Koo, S., Rho, J., & Lee, D. (2020). Laser digital patterning of conductive electrodes using metal oxide nanomaterials. Nano Convergence, 7(1), 1-17.

[27] Nam, V. B., Shin, J., Yoon, Y., Giang, T. T., Kwon, J., Suh, Y. D., ... & Lee, D. (2019). Highly Stable Ni-Based Flexible Transparent Conducting Panels Fabricated by Laser Digital Patterning. Advanced Functional Materials, 29(8), 1806895.

[28] Mizoshiri, M., & Kondo, Y. (2019). Direct writing of two-and three-dimensional Cu-based microstructures by femtosecond laser reductive sintering of the Cu 2 O nanospheres. Optical Materials Express, 9(7), 2828-2837.

[29] Nam, V. B., Shin, J., Choi, A., Choi, H., Ko, S. H., & Lee, D. (2021). High-temperature, thin, flexible and transparent Ni-based heaters patterned by laser-induced reductive sintering on colorless polyimide. Journal of Materials Chemistry C, 9(17), 5652-5661.

[30] Tumkin, I. I., Khairullina, E. M., Panov, M. S., Yoshidomi, K., & Mizoshiri, M. (2021). Copper and nickel microsensors produced by selective laser reductive sintering for non-enzymatic glucose detection. Materials, 14(10), 2493.

[31] Seiler, M., Knauft, A., Gruben, J. J., Frank, S., Barz, A., Bliedtner, J., & Lasagni, A. F. (2022). Modification of Polymeric Surfaces with Ultrashort Laser Pulses for the Selective Deposition of Homogeneous Metallic Conductive Layers. Materials, 15(19), 6572.

[32] Ratautas, K., Andrulevičius, M., Jagminienė, A., Stankevičienė, I., Norkus, E., & Račiukaitis, G. (2019). Laser-assisted selective copper deposition on commercial PA6 by catalytic electroless plating–Process and activation mechanism. Applied Surface Science, 470, 405-410.

[33] Khairullina, E. M., Ratautas, K., Panov, M. S., Andriianov, V. S., Mickus, S., Manshina, A. A., ... & Tumkin, I. I. (2022). Laser-assisted surface activation for fabrication of flexible non-enzymatic Cu-based sensors. Microchimica Acta, 189(7), 259.

[34] Xu, H., Zhang, J., Feng, J., & Zhou, T. (2021). Fabrication of copper patterns on polydimethylsiloxane through laser-induced selective metallization. Industrial & Engineering Chemistry Research, 60(24), 8821-8828.

[35] Zhang, J., Zhou, T., & Wen, L. (2017). Selective metallization induced by laser activation: fabricating metallized patterns on polymer via metal oxide composite. ACS Applied Materials & Interfaces, 9(10), 8996-9005.

[36] Xu, H., Feng, J., Yu, F., Huang, J., & Zhou, T. (2022). Laser-Induced Selective Metallization on Polymers for Both NIR and UV Lasers: Preparing 2D and 3D Circuits. Industrial & Engineering Chemistry Research.

[37] Jones, J., Snowdon, M. R., Rathod, S., & Peng, P. (2023). Direct laser writing of copper and copper oxide structures on plastic substrates for memristor devices. Flexible and Printed Electronics.

[38] Panov, M. S., Grishankina, A. E., Stupin, D. D., Lihachev, A. I., Mironov, V. N., Strashkov, D. M., ... & Ryazantsev, M. N. (2020). In situ laser-induced fabrication of a ruthenium-based microelectrode for non-enzymatic dopamine sensing. Materials, 13(23), 5385.

[39] Panov, M. S., Zakharov, A. P., Khairullina, E. M., Tumkin, I. I., Mereshchenko, A. S., Nikolaev, D. M., ... & Ryazantsev, M. N. (2022). Au–Ru Composite for Enzyme-Free Epinephrine Sensing. Chemosensors, 10(12), 513.

[40] Khairullina, E. M., Tumkin, I. I., Stupin, D. D., Smikhovskaia, A. V., Mereshchenko, A. S., Lihachev, A. I., ... & Panov, M. S. (2021). Laser-assisted surface modification of Ni microstructures with Au and Pt toward cell biocompatibility and high enzyme-free glucose sensing. ACS omega, 6(28), 18099-18109.

[41] Tumkin II, S. A. P. M., & IA, K. E. E. S. B. (2018). Ryazantsev MN Kochemirovsky VA In situ laser-induced codeposition of copper and different metals for fabrication of microcomposite sensor-active materials. Anal. Chim. Acta, 1044, 138-146.

[42] Shishov, A., Pochivalov, A., Nugbienyo, L., Andruch, V., & Bulatov, A. (2020). Deep eutectic solvents are not only effective extractants. TrAC Trends in Analytical Chemistry, 129, 115956.

[43] Brett, C. M. (2018). Deep eutectic solvents and applications in electrochemical sensing.

Current Opinion in Electrochemistry, 10, 143-148.

[44] Shishov, A., Gordeychuk, D., Logunov, L., Levshakova, A., Andrusenko, E., Chernyshov, I., ... & Tumkin, I. (2021). Laser-induced deposition of copper from deep eutectic solvents: optimization of chemical and physical parameters. New Journal of Chemistry, 45(46), 21896-21904.

[45] Avilova, E. A., Khairullina, E. M., Shishov, A. Y., Eltysheva, E. A., Mikhailovskii, V., Sinev, D. A., & Tumkin, I. I. (2022). Direct Laser Writing of Copper Micropatterns from Deep Eutectic Solvents Using Pulsed near-IR Radiation. Nanomaterials, 12(7), 1127.

[46] Sarma, U., & Joshi, S. N. (2022). Spatial and temporal thermo-physical analysis of Laser-induced plasma assisted ablation (LIPAA) of polycarbonate. Optics & Laser Technology, 150, 107908.

[47] Rahman, T. U., Rehman, Z. U., Ullah, S., Qayyum, H., Shafique, B., Ali, R., ... & Qayyum, A. (2019). Laser-induced plasma-assisted ablation (LIPAA) of glass: effects of the laser fluence on plasma parameters and crater morphology. Optics & Laser Technology, 120, 105768.

[48] Shuhao, C., Sergeev, M., Petrov, A., Varzhel, S., & Li, L. (2023). The fabrication processes and simple micro-cavity size adjustment of fiber Mach-Zehnder interferometer by laser-induced micro-plasma. Optical and Quantum Electronics, 55(4), 321.

[49] Wang, N., Zhao, L., Bai, J., Xu, J., He, Y., Dong, J., & Zhang, L. (2022, August). Research on Surface Metallization of Polyimide Film. In Journal of Physics: Conference Series (Vol. 2334, No. 1, p. 012010). IOP Publishing.

[50] Chen, J. J., An, Q., Rodriguez, R. D., Sheremet, E., Wang, Y., Sowade, E., ... & Feng, Z. S. (2019). Surface modification with special morphology for the metallization of polyimide film. Applied Surface Science, 487, 503-509.

[51] Liu, T. J., Chen, C. H., Wu, P. Y., Lin, C. H., & Chen, C. M. (2019). Efficient and adhesiveless metallization of flexible polyimide by functional grafting of carboxylic acid groups. Langmuir, 35(22), 7212-7221.

[52] Matula, R. A. (1979). Electrical resistivity of copper, gold, palladium, and silver. Journal of Physical and Chemical Reference Data, 8(4), 1147-1298.

[53] León, J. J. D., Fryauf, D. M., Cormia, R. D., & Kobayashi, N. P. (2016, September). Study of the formation of native oxide on copper at room temperature. In Low-Dimensional Materials and Devices 2016 (Vol. 9924, pp. 63-69). SPIE.

[54] Mahmoud, M. M. (2022). Characterization of the Native Oxide Shell of Copper Metal Powder Spherical Particles. Materials, 15(20), 7236.

[55] Zhu, Y., Mimura, K., Lim, J. W., Isshiki, M., & Jiang, Q. (2006). Brief Review of Oxidation Kinetics of Copper at 350 °C to 1050 °C. Metallurgical and materials transactions A, 37(4), 1231.

[56] Tylecote, R. F. (1950). THE OXIDATION OF COPPER AT 350-900 C. IN AIR. J Inst Met, 78, 327-350.